Supercond. Sci. Technol. 8 (1995) 558–563. Printed in the UK

Magnetic melt texturing combined with hot pressing applied to superconducting (2223) Bi–Pb–Sr–Ca–Cu–O ceramics

J G Noudem†, J Beille‡, E Beaugnon†, D Bourgault†, D Chateigner§, P Germi§, M Pernet§, A Sulpice† and R Tournier†

† EPM-MATFORMAG, Laboratoire d'Elaboration par Procédé Magnétique, Centre National de la Recherche Scientifique, BP 166, 38042 Grenoble Cédex 9, France
‡ Laboratoire Louis Néel, Centre National de la Recherche Scientifique, BP 166, 38042 Grenoble Cédex 9, France
§ Laboratoire de Cristallographie, Centre National de la Recherche Scientifique, BP 166, 38042 Grenoble Cédex 9, France

Received 26 April 1995

Abstract. We describe a new texturing process for superconducting ceramics which combines the effects of magnetic melt texturing (MMT) and hot pressing (HP), referred to in the following as the MMHPT process. This process essentially involves three steps: (i) a hot pressing at a temperature T_P, (ii) a partial melting in a magnetic field at a slightly higher temperature T_M, (iii) a second hot pressing at the same temperature T_P. Optimization of the thermomechanical treatment in a magnetic field applied to the (2223) Bi–Pb–Sr–Ca–Cu–O cuprates led to highly textured and dense samples carrying transport current density J_c of 3800 A cm^{-2} at 77 K in zero field.

1. Introduction

In view of industrial applications, the superconducting cuprates have to be processed so as to align their constituent grains and to improve connexions between them. A possible texturing technique which has been frequently used up to now is based on crystal growing in a liquid phase controlled by a thermal gradient [1] or by a magnetic field: magnetic melt texturizing (MMT), zone melting [2,3], etc. Another technique uses the effect of pressure at low temperature followed by a restoring annealing or the effect of pressure directly applied at high temperature: hot pressing (HP) [4–10].

In previous works, we have demonstrated that it was possible to texture Bi-based cuprates by MMT as well as by HP [11, 12, 13].

We have developed an apparatus combining both effects induced by hot pressing and crystal growing in a magnetic field in partially melted samples, constituting an original process we call magnetic melt and hot pressing texturizing (MMHPT). In this work, we have used our set-up to texture (2223) Bi–Pb–Sr–Ca–Cu–O ceramics. We first present the characteristics of the thermal cycle and the associated sequence of application of pressure and magnetic field. In a second part, we present physical measurements characterizing the texture degree and the electrical transport properties.

2. Experimental details

2.1. Apparatus

An experimental set-up allowing heating of samples to 1100 °C under an uniaxial maximum pressure of 60 MPa and in a magnetic field of 8 T has been built. This set-up has already been described in [11]. The heart of the system is made of two alumina push rods acting on the sample, inside a furnace located in a stainless steel water cooled chamber. The starting sample is a pellet 20 mm in diameter and 6 mm thick. Pressure is applied to the alumina pushing rods by steel pistons activated by a hydraulic jack. The active part of the set-up lies in a vessel allowing treatment in a controlled atmosphere and fitting in the room temperature bore of an 8 T superconducting coil.

This apparatus allows the use of uniaxial pressure to align platelets of a ceramic powder and to increase its density by suppressing voids between grains, especially at high temperature. It also allows a combination of these effects with partial melting in a magnetic field, which can increase the degree of orientation and grain size.

In this paper, results obtained by texturing (2223) Bi–Pb–Sr–Ca–Cu–O ceramics with this experimental set-up are presented. The starting precursors are (grade 2) $Bi_{1.6}Pb_{0.4}Sr_{1.6}Ca_{2.0}Cu_{2.8}O_{9.2+x}$ Hoechst powders.

0953-2048/95/070558+06$19.50

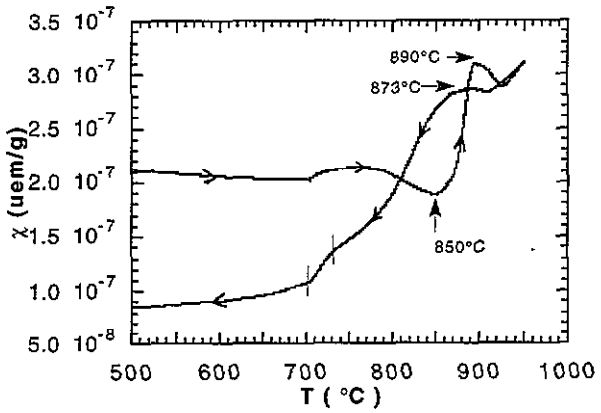

Figure 1. Thermal cycle of high-temperature magnetic susceptibility of (2223) Bi–Pb–Sr–Ca–Cu–O ceramic.

2.2. Initial compacting and pre-sintering

The powder is first pelletized under a 1 GPa pressure using a compacting cell. The initial dimensions of the pellet are a diameter of 20 mm and a thickness of 6 mm. The pellets are then annealed in air at 840 °C for 90 hours.

3. Preliminary determination of the melting interval

Information on the physical state of the sample during the thermal treatment is obtained from *in situ* magnetic susceptibility measurements according to a technique developed in the EPM-MATFORMAG laboratory [14]. The sample placed in an alumina crucible located in a magnetic field gradient $\partial H/\partial z$ is submitted to a magnetic force $F = -\chi H \partial H/\partial z$ which can be measured by a microbalance. Figure 1 shows a typical magnetic susceptibility curve of (2223) Bi–Pb–Sr–Ca–Cu–O. This curve shows a minimum around 850 °C that corresponds to the beginning of melting in agreement with the phase diagram proposed in [15]. The increase of susceptibility between 850 and 890 °C is related to the phases formed. Melting ends near 890 °C, where a maximum of susceptibility is observed. Above 890 °C, the susceptibility strongly decreases with temperature in a way very similar to the case of Y–Ba–Cu–O [14]. This susceptibility variation is probably associated with a lowering of oxygen stoichiometry yielding partial reduction of Cu^{2+} to non-magnetic Cu^{+}. The susceptibility curve exhibits a hysteretic behaviour with decreasing temperature.

4. Thermomechanical treatment in a magnetic field

We have used the previous high-temperature magnetic susceptibility results to determine the characteristics of the heat treatment that we describe in figure 2.

We first induce a preorientation of the platelets by applying a uniaxial stress of 28 MPa for 5 hours at a temperature $T_p = 855$ °C, at which a minimum amount of liquid phase is expected. In a preceding paper [12], we reported that pressure applied at 857 °C leads to the expulsion of a Bi-rich liquid phase. At 855 °C, we think that creep is limited by the presence of a solid 'skeleton'.

At the end of the preorientation step, pressure is released and a magnetic field of 8 T applied. Melting increases in the sample up to a second plateau at a temperature T_M . This temperature has to be high enough so as to allow magnetic field to be efficient but not too high to prevent the occurence of excessive secondary phases. We have optimized the value of the temperature T_M in the range 855–870 °C. The high-temperature step is followed by a slow cooling ramp of 0.5 °C h^{-1} intended for magnetic field-oriented solidification down to 855 °C, at which temperature the field is turned off.

During a third dwell at 855 °C, a pressure of 28 MPa is again applied for 5 hours. The aim of this step is to enhance the density, suppress the voids and increase the connections between grains. This pressure is removed at the end of a cooling ramp of 5 °C h^{-1} down to 800 °C. Maintaining pressure below this temperature results in several cracks in the pellet.

5. Characterization

5.1. Scanning electron microscopy

Figure 3 shows a micrograph picture of a broken face of an MMMHPT (2223) Bi–Pb–Sr–Ca–Cu–O pellet parallel to the pressure and magnetic field axis. A high degree of orientation is observed. Moreover, excellent intergrain connection in the whole sample will be proved in the following by measurements of critical current densites. The platelets are approximately 20 μm long. Some voids can be detected, which probably could be avoided by an optimized MMHPT process. Our samples processed in the partial melting temperature range have high density of 6.1 g cm^{-3} which can be compared to the theoretical one of 6.2 g cm^{-3}.

5.2. Texture analysis by x-ray pole figures

A classic θ–2θ scan has been first recorded on a face perpendicular to the direction of the stress and magnetic field applied during processing which shows very strong (00*l*) reflections (figure 4). This can be taken as an indication that the experimental process tends to align the *c* axis of crystallites following a preferential axial direction. Weak (*hkl*) components are also observed showing traces of a small proportion of scattered crystallites. However, a quantitative and qualitative determination of texture cannot be accurately determined with such a spectrum, and we then decided to obtain x-ray diffraction pole figures. Measurements were carried out using a four-circle diffractometer operating in the Schulz reflection geometry [16] and a Rigaku rotating anode generator, and using the Cu Kα radiation monochromatized by the (002) reflection of a flat graphite single crystal. The pole figure was analysed throughout the azimuthal angle φ in the region $0 \leq \varphi \leq 360°$ and throughout the tilt angle α in the interval $0 \leq \alpha \leq 72$ with steps of 3.6° and 1.8° respectively. Corrections for background and defocusing, and normalization were realized by standard procedures [17,18] using our own programs (CORTEXG and POFINT).

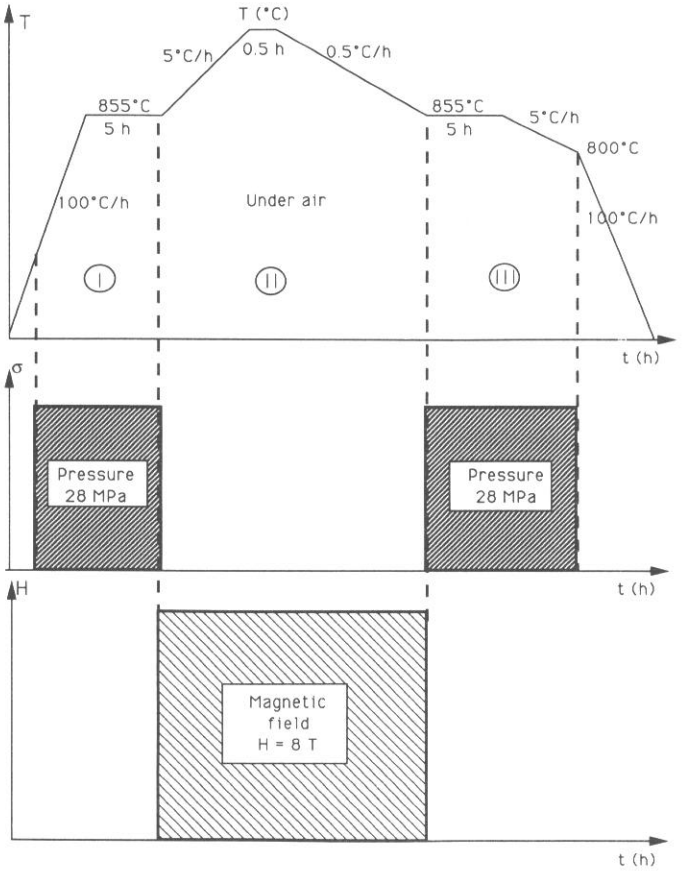

Figure 2. Processing thermal cycle and associated diagram of pressure and magnetic field application.

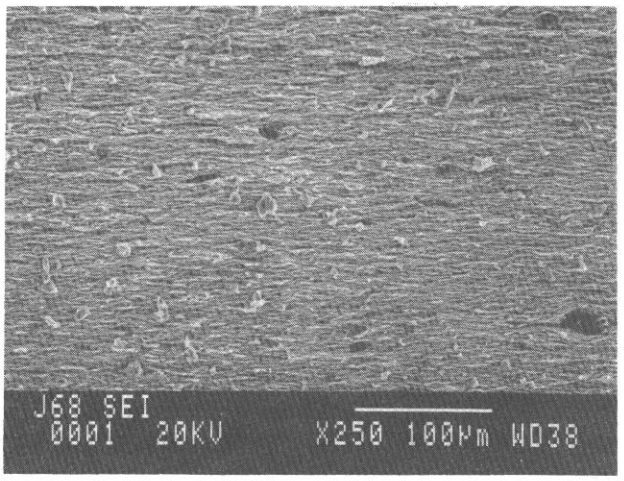

Figure 3. SEM micrograph picture of a processed MMHPT (2223) Bi–Pb–Sr–Ca–Cu–O pellet face broken parallel to the applied stress and magnetic field direction.

Figure 5 represents the {0014} experimental pole figure measured on the same face as that of figure 4. The central pole of this figure denotes a relatively high degree of preferred orientation of crystallites with their *c* axes parallel to the texturing direction and with a dispersion up to 25° from this direction (which coincides with the intensity axis), at 10% of the maximum intensity. This dispersion is to be compared with the broadening of the curves of critical current density as a function of the tilting angle between the preferential axis and the magnetic field (figure 8 and 9). In comparison, textured YBaCuO samples exhibit a higher degree of texturizing and narrower J_c peaks [19].

The maximum (00*l*) pole density is of approximately 3.5 m.r.d. (multiple of random distribution), estimated from the pole figure. The increasing level in the higher analysed α region comes from the {020} and {200} reflections because of defocusing of the x-ray beam at the surface of the sample. In the middle α region, randomly oriented crystallites (also detected in the θ–2θ scan) are responsible for a constant diffracting intensity over the whole pole figure which accounts for the non-zero level. A {117} pole figure has been also carried out. It shows a ring shape, from which we could deduce that *a* and *b* axes are randomly distributed around the preferential direction.

5.3. Magnetic measurements

In order to correlate the texture to the magnetic anisotropy, hysteresis magnetic cycles with measuring magnetic fields applied parallel and perpendicular to the direction of stress and magnetic field used during processing have been measured at 4.2 K. Results shown in figure 6 indicate a maximum value of approximately four for the anisotropy factor. This factor is larger than previous values of two to three obtained in processes involving hot pressing or magnetic melt texturizing separately [13].

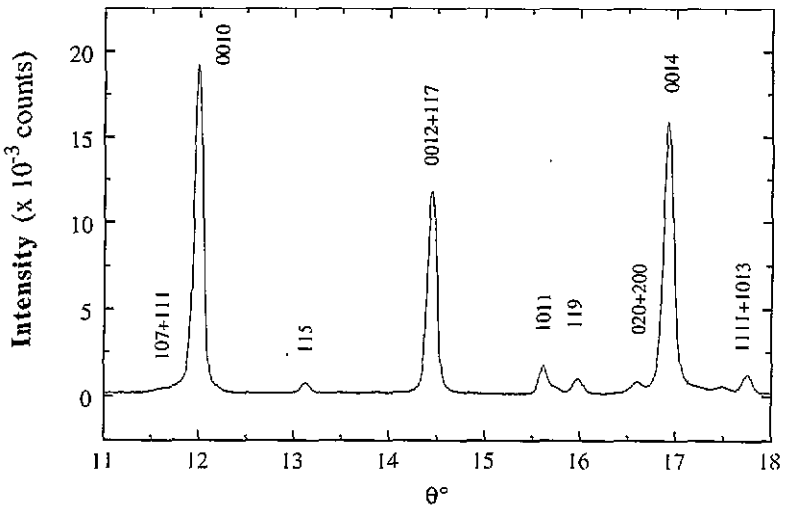

Figure 4. θ–2θ spectrum in the $11° \leq \theta \leq 18°$ range. Notice the (00*l*) enhanced reflections which denote the preferential (00*l*) orientation.

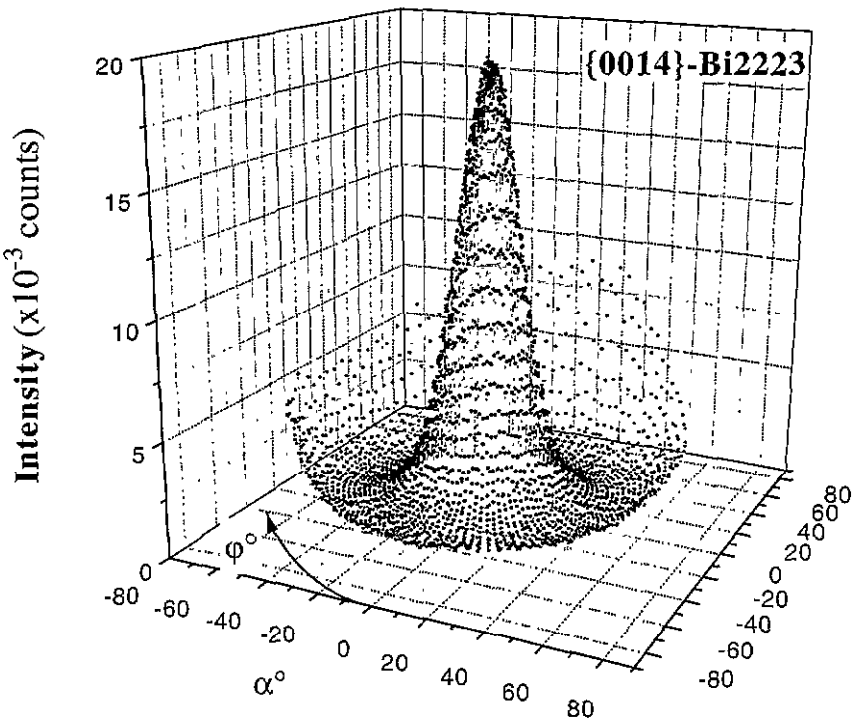

Figure 5. {0014} experimental pole figure of the Bi–Pb–Sr–Ca–Cu–O (2223) sample revealing the *c* axis dispersion.

5.4. Transport properties and critical current densities

The temperature T_M of the plateau of partial melting under magnetic field has been optimized between 855 and 870 °C from values of transport critical current densities J_c at 77 K in zero field. Measurements of J_c were made using a four-points technique with an electric field criterion of 10 μV cm^{-1}. A maximum J_c value of 3800 A cm^{-2} has been obtained for T_M = 860 °C, as deduced from figure 7, which corresponds to the optimum temperature of the process. The decrease in the critical current density at T_M > 860 °C can be correlated with the presence of secondary $(Ca–Sr)_{14}Cu_{24}O_x$, CuO, $(Ca–Sr)_2CuO_3$ phases that we have detected by semiquantitative SEM analysis. The maximum J_c value can be compared to 1500 and 2500 A cm^{-2} obtained with process of magnetic melt texturizing and hot pressing alone [13]. We have to notice that the J_c value of 3800 A cm^{-2}, which can appear as comparable to hot pressed samples only, is obtained for thick samples of $\simeq$1 mm cut in pellets 3.5 mm thick. It is known that in weak-critical-field superconductors, the current density is limited by the self-field at the surface of the superconductor. This explains the fact that in the Bi–Pb–Sr–Ca–Cu–O ceramics the J_c measured values depend on the thickness of the sample and are weaker for thicker

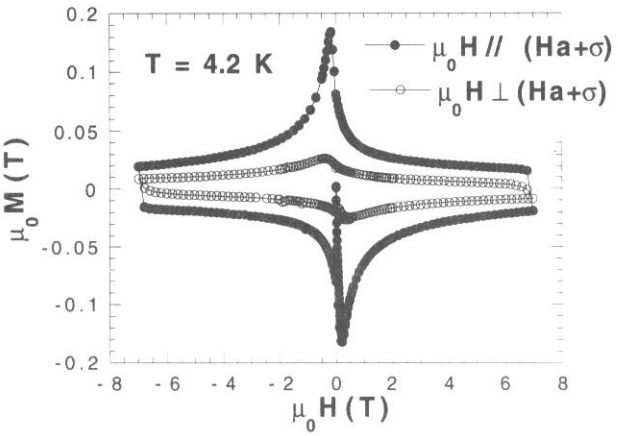

Figure 6. Magnetic hysteresis cycle following two directions of the measuring magnetic field parallel and perpendicular to the synthesis stress and magnetic field.

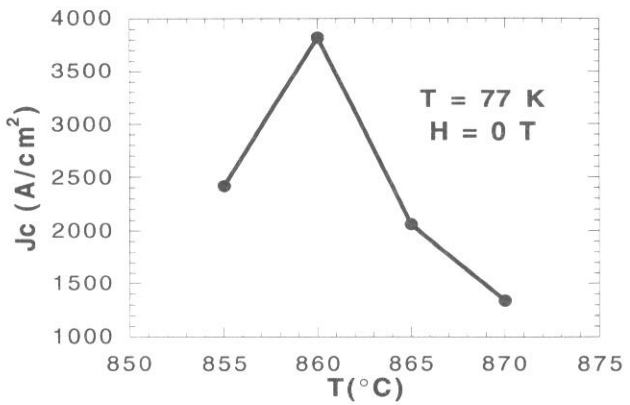

Figure 7. Transport current density versus temperature T_M of partial melting under field at 77 K and without field.

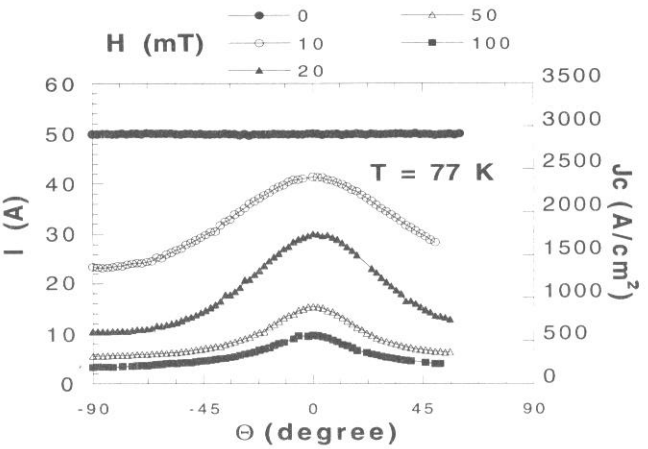

Figure 8. Transport critical current perpendicular to the synthesis stress and magnetic field as a function of the tilting angle around the current direction.

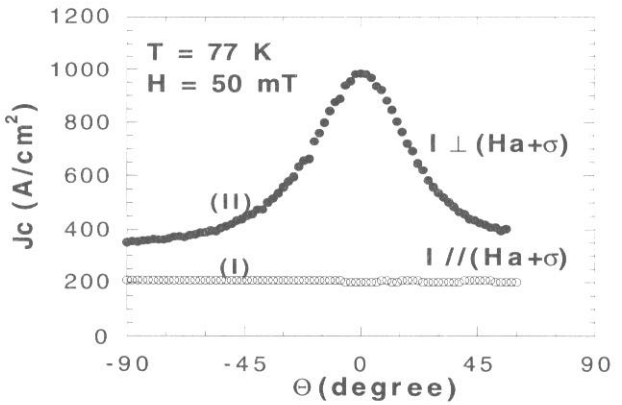

Figure 9. Curves of transport critical current versus rotating angle for bars of processed samples cut parallel to the synthesis stress and magnetic field (I) and perpendicular to this direction (II).

samples [20] as in our case. The largest J_c values of $\simeq$50 kA cm^{-2} obtained in the Bi–Pb–Sr–Ca–Cu–O powder in tube samples [21] are measured in specimen of a few tens of micrometers thick. Moreover, in these silver sheathed tapes surface pinning may favour much higher critical current density.

It can be noted that the texture of the samples can also be deduced from the angular dependence of the transport critical current under magnetic field. Figure 8 shows critical current measurements obtained in a configuration where the current flows perpendicular to the texture direction, the magnetic field is perpendicular to the current axis and the sample is rotating around the current axis. For a given orientation of the texture direction with respect to the field, the critical current is a decreasing function of the field. For a given field, the critical current goes through a maximum at $\theta = 0$ (magnetic field perpendicular to the texture direction), which means that crystallites are preferentially oriented with their c axis parallel to the texture direction.

In order to establish whether our samples could sustain sizeable currents in the direction (uneasy) of applied stress and magnetic field, we have cut bars following this uneasy direction (I) and in the perpendicular easy one (II). The curves of critical current corresponding to these two directions as a function of the rotating angle around the current axis for the same magnetic field of 50 mT are presented in figure 9. We do note that (i) sample (I) can carry a rather large critical current density of 200 A cm^{-2} at 77 K and in 50 mT (the corresponding critical current density is 1000 A cm^{-2} at 77 K and under zero field), (ii) the curve of sample (I) as a function of rotating angle is flat compared to the one of sample (II) demonstrating that the platelets are very well c-axis oriented parallel to the direction of the applied stress and magnetic field. Comparison of the two curves gives a maximum anisotropy factor of about five. This value is larger than the J_c anisotropy of about two found for (2223) Bi–Pb–Sr–Ca–Cu–O treated by hot pressing only [12] which points out the interest of the MMHPT process.

The normal state resistivities of the two samples (I) and (II) exhibit a large anisotropy ratio of about 11 at 300 K as can be deduced from figure 10, much larger than the factor of five found for (2223) Bi–Pb–Sr–Ca–Cu–O treated by hot pressing only.

It seems not obvious that at 860 °C, where a little liquid is expected, the magnetic field can have a sizeable effect. Indeed, other researchers have reported beneficial effects of short excursions above the partial melting temperature of (2223) Bi–Pb–Sr–Ca–Cu–O [22, 23]. To point out the

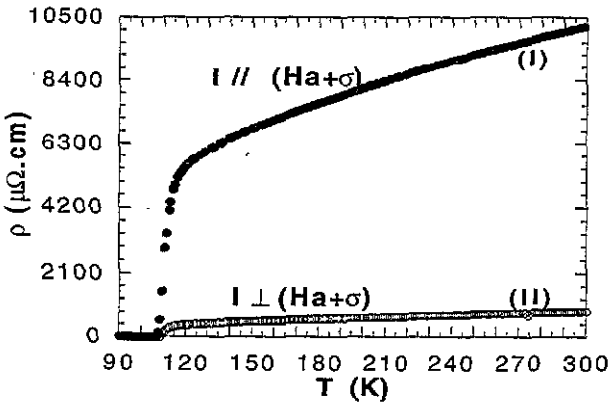

Figure 10. Thermal dependence of the normal state resistivity of bars (I) and (II).

effect of magnetic field, we have realized the MMHPT process without magnetic field but with the step of melting at 860 °C. Samples obtained from this process exhibited a J_c of only 2500 A cm^{-2}, which is the value obtained by hot pressing only. To further elucidate the effects of magnetic field, we intend to examine partially processed specimens: after the first hot pressing, after the partial melting and magnetic alignment.

6. Conclusion

The process combining a thermomechanical cycle with a partial melting in a magnetic field (MMHPT) seems to be very promising. The quality of the texture has been improved as compared to the samples processed by hot pressing (HP) or partial melting in a magnetic field (MMT) separately. The texture degree has been quantified in this paper by means of SEM micrography, x-ray pole figures, magnetic hysteresis and electrical transport properties. Moreover, the transport critical current density has been increased with respect to HP or MMT and we obtained 3800 A cm^{-2}.

We think that these results obtained in a first optimization step can be improved in view of the large number of parameters of the process: length and temperature of the HP and MMT dwells, slope of solidification ramp, controlled atmosphere etc and this opens interesting perspectives.

Acknowledgments

JGN acknowledges his fellowship from ADEME and Alcatel Alsthom. This work is supported by the CPR on superconductivity of PIRMAT. We warmly thank M Bonvalot for useful discussions and very careful reading of the manuscript. We are grateful to P Amiot for her help in carrying out the SEM studies.

References

[1] Jin S, Tiefel T M, Sherwood R C, Van R B Dover, Davis M E, Kammlott G W and Fastnacht R A 1987 *Phys. Rev.* B **37** 7850
[2] Lees M R, P. de Rango, Bourgault D, Barbut J M, Braithwaite D, Lejay P, Sulpice A and Tournier R 1992 *Supercond. Sci. Technol.* **5** 362
[3] Barbut J M, Barrault M, Boileau F, Ingold M, Bourgault D, de Rango P and Tournier R 1993 *Appl. Supercond.* (DGM :Eucas-Göttingen) vol 1 p 345
[4] Ito A, Matsuda M, Iwai Y, IshII M, Takata M, Yamashita T and Koinuma H 1989 *Japan. J. Appl. Phys.* **28** L380
[5] Asano T, Tanaka Y, Fukutomi M, Jikihara K and Maeda H 1989 *Japan. J. Appl. Phys.* **28** L595
[6] Haldar P, Hoehn J G Jr and Rice J A 1992 *Appl. Phys. Lett.* **60** 495
[7] Ikeda H, Yoshizaki R, Yoshikawa K and Tomita N 1990 *Japan. J. Appl. Phys.* **29** L430
[8] Yoshizaki R, Ikeda H, Yoshikawa K and Tomita N 1990 *Japan. J. Appl. Phys.* **29** L753
[9] Tampieri A and Babini G N 1991 *Japan. J. Appl. Phys.* **30** L1163
[10] Gao W and Vander J B Sande 1992 *Supercond. Sci. Technol.* **5** 318
[11] Noudem J G, Beille J, Draperi A, Sulpice A and Tournier R 1993 *Supercond. Sci. Technol.* **6** 795
[12] Noudem J G, Beille J, Bourgault D, Sulpice A and Tournier R 1994 *Physica* C **230** 42
[13] Noudem J G, Beille J, Bourgault D, Sulpice A and Tournier R 1995 *M^{2}S-HTSC IV, Int. Conf. (Grenoble, July 1994) Physica* C to appear
[14] de Rango P, Chaud X, Gautier P, Beaugnon E and Tournier R 1993 *Applied Superconductivity* (DGM: Eucas-Göttingen) vol 1 305
[15] Strobel P, Tolédano J C, Morin D, Schneck J, Vacquier G, Monnereau O, Primot J and Fournier T 1992 *Physica C* **201** 27
[16] Schulz L G 1949 *J. Appl. Phys.* **20** 1030
[17] Holland J R 1964 *Adv. X-ray Anal.* **7** 86
[18] Chateigner D, Germi P and Pernet M 1992 *J. Appl. Cryst.* **25** 766
[19] Bourgault D, Barbut J M, Ayache J, Chateigner D, Tournier R, Gotor F J, Bahezre C, Germi P and Pernet M 1994 *M^{2}S-HTSC IV, Int. Conf. (Grenoble, July 1994) Physica C* **235–240** 567
[20] Venugopal K and Swaminathan G 1994 *Cryogenics* **34** 325
[21] Ueyama M, Hikata T, Kato T and Sato K 1991 *Japan. J. Appl. Phys.* **30** L1384
[22] Dou S X, Liu H K and Guo Y C 1992 *Appl. Phys. Lett.* **60** 2929
[23] Majewski P, Kaesche S, Aldinger F, Elschner S, Hettich B and Lang C 1993 *Applied Superconductivity* (DGM: Eucas-Göttingen) vol 1 129